RESEARCH

Rice yellow stunt virus p3 protein enters the nucleus of leafhopper cell and localizes to viroplasm through interaction with N protein via importin α3-mediated pathway

Zhejun Huang[1], Zhenxi Ji[1], Juan Wang[1], Zhanpeng Li[1], Zhoumian Jiang[1], Wei Ni[1], Hongyan Chen[1], Taiyun Wei[1*] and Xiao-Feng Zhang[1*]

Abstract

Rice yellow stunt virus (RYSV) P3 protein functions as a movement protein during viral infection of a plant host; its function in insect hosts remains unclear. In this study, we investigated the subcellular localization of P3 using leafhopper (*Nephotettix cincticeps*) cell cultures. Our results showed that P3 translocated from the cytoplasm to the nucleus in RYSV-infected leafhopper cells, where it interacted with the viral N protein as a constituent of viroplasms. Interfering with the *P3* gene expression significantly suppressed viral infection in *N. cincticeps*. Finally, we demonstrate that the nuclear translocation of P3 in leafhopper cells depended on its interaction with RYSV N protein, which enters the nucleus via an interaction with importin α3. These findings unveil a previously unknown role for P3 in RYSV infection of the insect vector and provide valuable insights into the infection dynamics of plant rhabdoviruses.

Keywords Rice yellow stunt virus, P3 protein, Viroplasm, Importin α3, Insect vector

Background

Plant rhabdoviruses infect numerous dicotyledons and monocotyledons and rely on transmission by hemipteran insects, including aphids, planthoppers, and leafhoppers (Hogenhout et al. 2008; Kormelink et al. 2011; Mann et al. 2014; Kuhn et al. 2020). Some of these viruses cause substantial economic losses in agriculture and aquaculture. Plant rhabdoviruses exhibit a dual-host lifecycle as obligatory inhabitants of plants and insects (Kuzmin et al. 2009). Due to the structural, physiological, and biochemical differences between plant and insect cells, the proteins encoded by plant rhabdoviruses may serve distinct functions in these two host types. Recent advances in the field of plant rhabdovirus research have been notable, marked by the successful development of infectious clones for these viruses (Wang et al. 2015; Gao et al. 2019). This accomplishment has yielded a crucial tool for investigating the functionalities of proteins encoded by plant rhabdoviruses, utilizing reverse genetics methods. Numerous novel functions of various proteins from plant rhabdoviruses have emerged during viral infection in host plants (Zhou et al. 2019; Ding et al. 2022; Fang et al. 2022; Gao et al. 2022). However, to date, little is known about the roles of virus-encoded proteins from plant rhabdoviruses in the infection of insect vectors.

*Correspondence:
Taiyun Wei
weitaiyun@fafu.edu.cn
Xiao-Feng Zhang
zhangxiaofeng911@163.com
[1] State Key Laboratory of Ecological Pest Control for Fujian and Taiwan Crops, Institute of Plant Virology, Fujian Agriculture and Forestry University, Fuzhou 350002, Fujian, China

Yellow stunt disease of rice (*Oryza sativa*) was initially reported in Taiwan province and was subsequently observed in other southern regions of China and in Japan and Thailand (Wang et al. 2018). The distinctive symptoms of this disease include progressive leaf yellowing from the leaf tip towards the leaf base with maintenance of green coloration in leaf veins. Affected plants exhibit severe stunting and a significant reduction in tillering (Cheng et al. 1992). The causal agent for yellow stunt disease is rice yellow stunt virus (RYSV, *Alphanucleorhabdovirus oryzae*), an alphanucleorhabdovirus that is persistently transmitted by the insect vectors *Nephotettix nigropictus*, *N. cincticeps*, and *N. virescens* (Wang et al. 2018). The complete genome of RYSV is approximately 14,000 nucleotides long and contains seven open reading frames (ORFs) arranged as follows: 3′N-P-3-M-G-6-L5′. These ORFs encode seven proteins: nucleoprotein (N), phosphoprotein (P), matrix protein (M), glycoprotein (G), large RNA polymerase (L), and the accessory proteins P3 and P6 (Fang et al. 1994; Huang et al. 2003, 2005; Guo et al. 2013; Jackson and Li 2016).

We previously investigated the roles of RYSV-encoded proteins in viral infection of leafhoppers and determined that N and P proteins are components of viral replication complexes within insect cells (Wang et al. 2018). Moreover, we observed that the matrix protein M interacts with actin, facilitates viral neurotropism in insects, and modulates polyamine synthesis in leafhoppers to enhance viral proliferation (Zhang et al. 2021). Additionally, our research revealed that the accessory protein P6 is an integral component of the viral replication complex that actively participates in its formation within leafhopper cells (Zhang et al. 2018). The function of P3 protein in viral infection of insects remains largely unexplored.

Gene 3 in the genomes of several plant rhabdoviruses, including RYSV, encodes a cell-to-cell movement protein (MP) which is essential for viral infection in plant hosts (Huang et al. 2005). Analysis of the primary and secondary protein structures of RYSV P3 showed that this protein should be a member of the '30 K' superfamily (Melcher 2000). Expressing RYSV P3 functionally complements the cell-to-cell movement of a movement-deficient mutant of potato virus X in *Nicotiana benthamiana* leaves (Zhou et al. 2019). Furthermore, RYSV P3, together with N, is a key component of the ribonucleocapsid involved in the intercellular movement of plant rhabdoviruses, highlighting its importance in viral dissemination within plants (Zhou et al. 2019). The distinct movement mechanisms exhibited by RYSV in plant and animal cells, coupled with the inherent physiological differences in cellular structures between these two types of organisms, suggest that P3 may possess additional functions beyond its role as a MP in insect cells.

In this study, we employed the RYSV/*N. cincticeps* infection system to elucidate the functions of P3. Our investigations revealed that P3 serves as a constituent of viroplasms. P3 interacts with N, which exploits the importin system to facilitate its entry into the insect cell nucleus. Suppression of either *P3* or *importin α3* gene expression substantially inhibits RYSV infection in insects. These findings unveil a novel role for P3 during RYSV infection of insect cells, shedding new light on the process of plant rhabdovirus infection.

Results

Subcellular localization of P3 in *N. cincticeps* cells

We investigated the subcellular localization of the RYSV P3 using a construct harboring *P3* driven by the *N. cincticeps Actin* promoter to express green fluorescent protein (GFP)-fused P3. We transfected vector cell monolayers (VCMs) with this construct and performed immunofluorescence analysis, finding that transiently expressed P3-GFP accumulated in punctate structures within the cytoplasm (Fig. 1a). To verify the subcellular localization of P3 during RYSV infection of *N. cincticeps* cells, we infected VCMs with RYSV at different time points, fixed the VCMs, and labeled them with a P3-specific antibody conjugated with fluorescein isothiocyanate (FITC) for immunofluorescence microscopy. At 18 h post infection (hpi), P3 was detected in the cytoplasm, with dispersed fluorescent signals. At 36 hpi, P3 fluorescence exhibited a continuous ring-like pattern around the nuclear membranes of 95% RYSV infected cells. At 48 hpi, abundant fluorescent signals were observed in the nuclei of RYSV-infected *N. cincticeps* cells (86%), where punctate spots gathered. At 72 hpi, P3 accumulated in the nucleus, and the fluorescence intensity was notably higher than at 48 hpi. Healthy control cells showed no fluorescence (Fig. 1b). Immunoelectron microscopy further revealed that P3 localized to electron-lucent inclusions known as viroplasm-like structures (Fig. 1c). These findings suggest that P3 is initially present in the cytoplasm and subsequently translocates into the nucleus to participate in the assembly of viroplasms during RYSV infection.

RYSV P3 enters the nucleus by interacting with N

To clarify the role of P3 in the assembly of RYSV viroplasms, we examined the interactions of P3 with the major components of RYSV viroplasms (N and P), two structural proteins (M and G), P6 and RNA polymerase (L) via yeast two-hybrid assays in yeast strain AH109. Only yeast cells containing the plasmids AD-N/BD-P3 and AD-M/BD-P3 grew on SD/−Trp/−Leu/−His/−Ade medium (Fig. 2a), indicating that P3 interacts with N and M. This interaction was confirmed in a GST pull-down assay, in which P3 strongly interacted with N
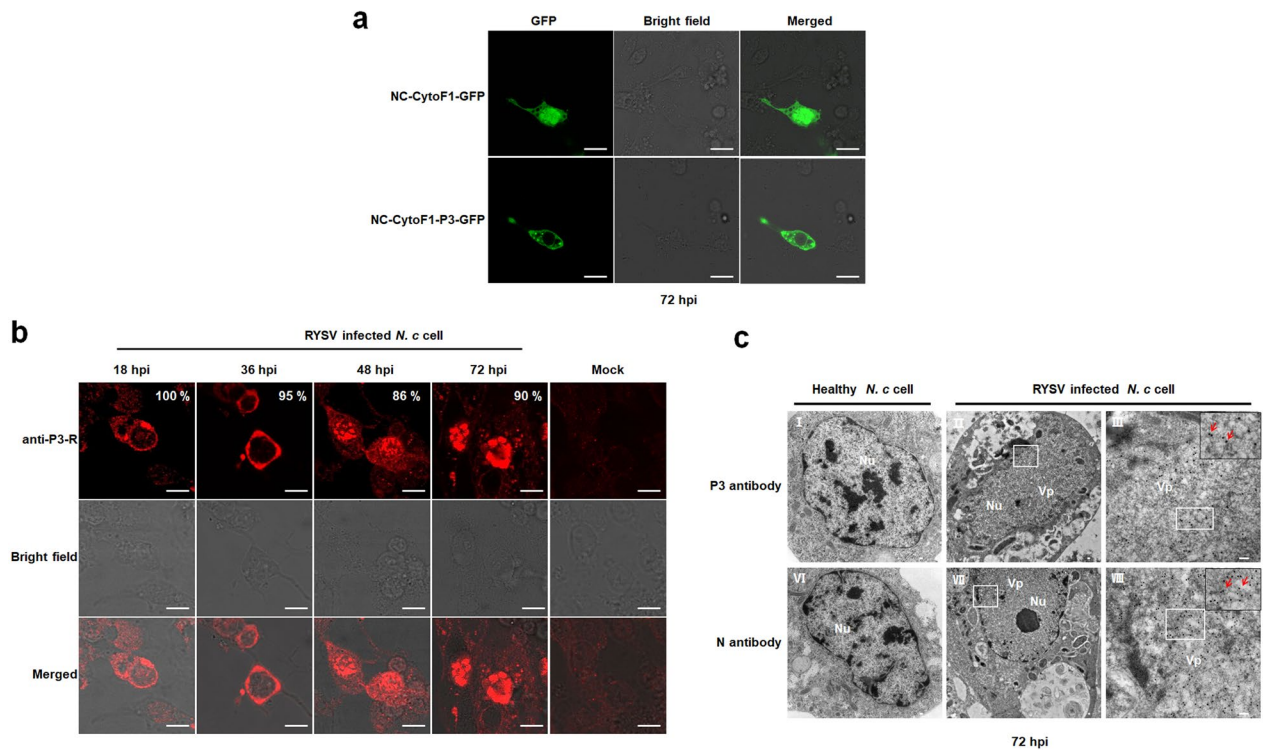
Fig. 1 Subcellular localization of RYSV nonstructural protein P3 in *N. cincticeps* VCMs. **a** Fluorescence of *N. cincticeps* cells expressing GFP fused to P3. *N. cincticeps* cells transfected with the NC-CytoF1-GFP vector served as a control. Scale bars: 20 μm. **b** Confocal immunofluorescence micrographs showing the cellular localization of RYSV P3 in *N. cincticeps* cells at different stages of RYSV infection. Infected VCMs at 18, 36, 48, and 72 hpi were immunolabeled with P3-specific IgGs directly conjugated to rhodamine. Scale bars: 20 μm. **c** Electron micrographs showing the subcellular localization of RYSV P3 in RYSV-infected VCMs. Samples were immunolabeled with P3-specific antibodies as primary antibodies and treated with goat-anti-rabbit IgG conjugated to 15-nm-diameter gold particles as secondary antibodies. RYSV-infected VCMs were labeled with N-specific antibody separately as a control. Scale bars: 100 nm

and M (Fig. 2b and Additional file 1: Figure S1). These results indicate that RYSV P3 directly interacts with RYSV N and M in vitro.

Since previous studies demonstrated that RYSV N contains a nuclear localization signal (NLS) and localizes to the nucleus in insect cells, we speculate that the localization of P3 in the nucleus might be due to its interaction with N. To test this hypothesis, we expressed N and P3 in Sf9 cells using the baculovirus expression system and examined the cells by immunofluorescence microscopy. P3 localized within the cytoplasm of Sf9 cells when expressed alone. However, when co-expressed with N, P3 co-localized with N within the nucleus (Fig. 2c). These results suggest that P3 enters the nucleus via its interaction with N.

To visualize the localization of N and P3 during RYSV infection, we labeled RYSV-infected VCMs with a P3-specific antibody conjugated to FITC and an N-specific antibody conjugated to rhodamine, and examined them by immunofluorescence microscopy. The results showed that during the early stages of RYSV infection, P3 co-localized with N in the cytoplasm. Notably,

we observed more fluorescent signals from GFP-fused N than from P3 at the onset of infection. Subsequently, between 36 and 72 hpi, the viroplasm structures formed by N and P3 accumulated in the nuclei of VCMs (Fig. 2d). These results indicate that during RYSV infection, P3 enters the nucleus by interacting with N and participates in the assembly of the viroplasm.

## Knocking down P3 inhibits RYSV infection in VCMs and insect cells

To investigate the role of P3 in RYSV infection in *N. cincticeps* cells, we employed RNA interference (RNAi) to knock down P3 expression. Double-stranded (ds) P3 or dsGFP RNA was transfected into RYSV-infected *N. cincticeps* VCMs using Cellfectin II. At 4 days post-transfection, the cells were fixed and immunolabeled with a specific antibody against RYSV. Confocal microscopy revealed a substantial reduction in fluorescent signals (approximately 25% of nuclei fluoresced; indicative of RYSV infection) in cells transfected with dsP3 compared to cells transfected with the control dsGFP (Fig. 3a). Furthermore, reverse transcription–quantitative PCR
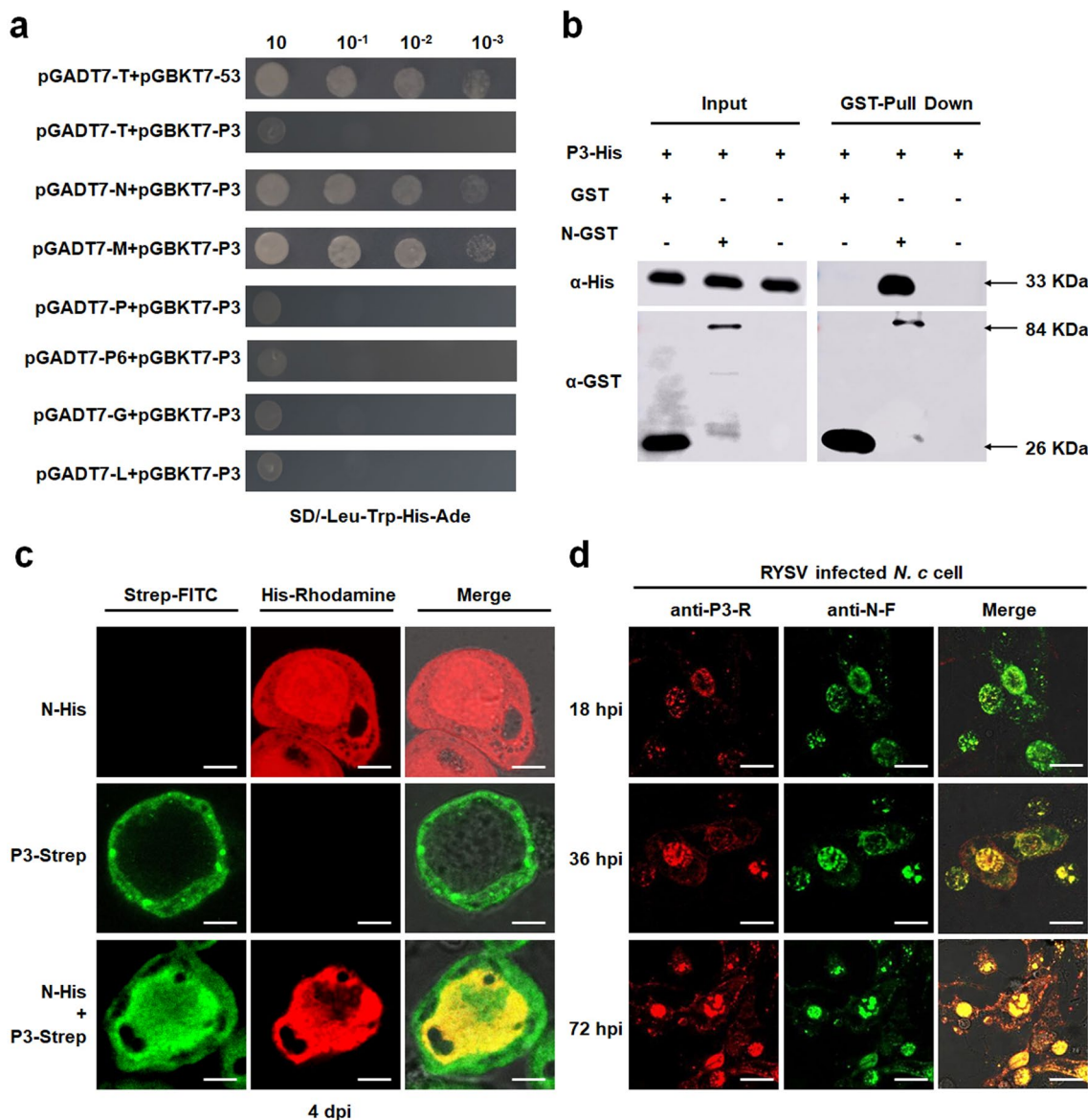
Fig. 2 In vitro and in vivo interactions of RYSV P3 and N. **a** Interactions between N and P3 in the yeast two-hybrid system. Yeast cells co-transformed with pGBKT7–53 and pGADT7-T were used as a positive control. **b** GST pull-down assay of the interaction of RYSV P3 with RYSV N. Bait protein N was fused with GST-tagged protein. Prey protein P3 was fused with His-tagged protein. Purified GST incubated with prey protein or purified His incubated with bait protein were used as controls. **c** Confocal immunofluorescence micrographs showing the colocalization of N-His and P3-Strep fusion proteins in Sf9 cells. Yeast cells expressing only N-His or P3-Strep served as a positive control. The samples were immunolabeled with Strep-tagged IgGs directly conjugated to FITC or His-tagged IgGs directly conjugated to rhodamine. Scale bars: 20 μm. **d** Confocal immunofluorescence micrographs showing the colocalization of N and P3 at different times after RYSV inoculation in host *N. cincticeps* cells. The cells were immunolabeled with N-specific IgGs directly conjugated to FITC or P3 specific IgGs directly conjugated to rhodamine. Scale bars: 20 μm

(RT-qPCR) and immunoblotting analyses confirmed that both the RNA and protein levels of N, P, P3, and M were significantly lower in cells treated with dsP3 than in cells treated with dsGFP; these results are consistent with those of the immunofluorescence assay (Fig. 3b, c). To rule out the possibility that small RNAs derived from dsP3 could directly silence the genomic RNA of RYSV, we prepared ds3'UTR RNA using a 300-bp fragment amplified from the 3'UTR of the RYSV genome, which is critical for the replication of RYSV genome. We transfected the ds 3'UTR into RYSV-infected cultured *N. cincticeps* cells. RT-qPCR assay results indicated that ds 3'UTR treatment did not affect the transcription of N, P, P3, and M from the RYSV genomic RNA (Additional
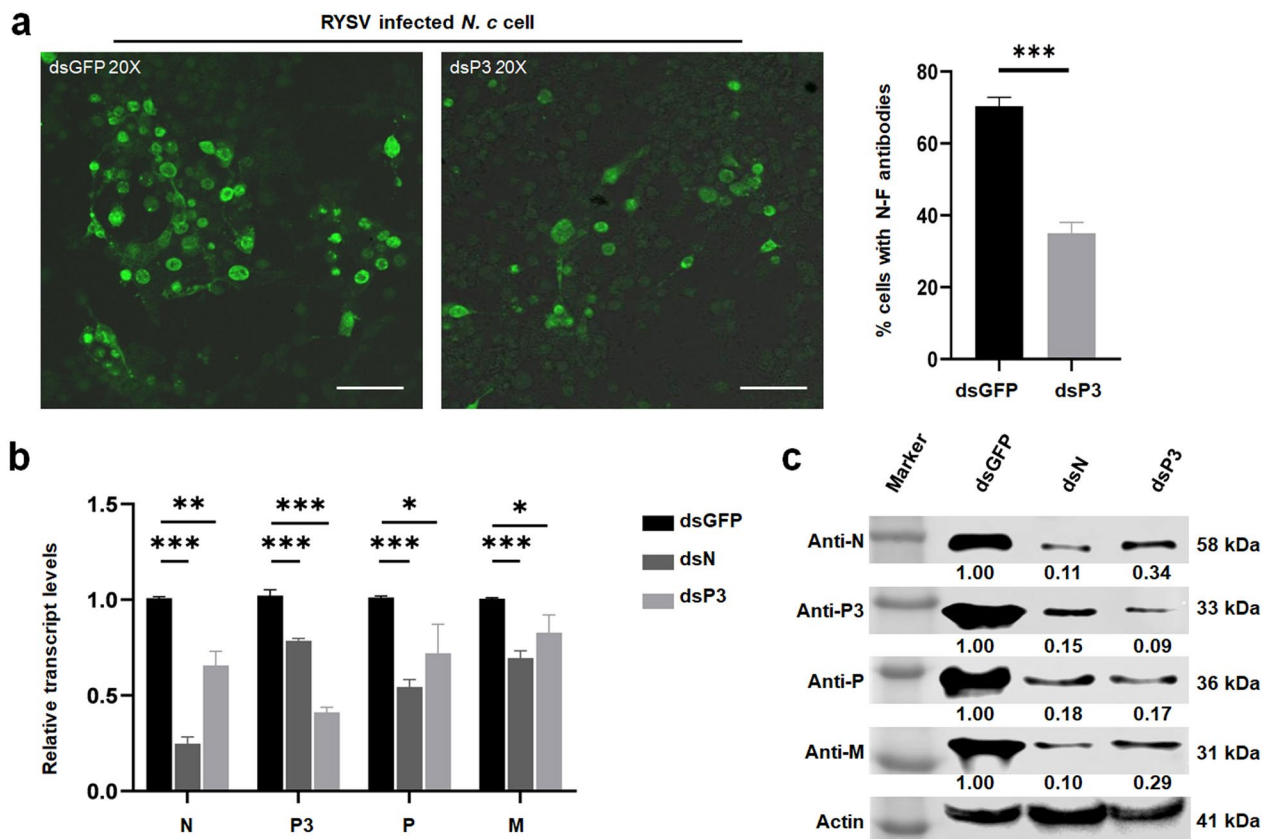
Fig. 3 Knockdown of *N* and *P3* by dsRNA treatment inhibits RYSV infection of VCMs. **a** VCMs were transfected with dsP3 or dsGFP and inoculated with RYSV. At 72 h post RYSV inoculation, the cells were immunolabeled with N-specific IgGs directly conjugated to FITC. Scale bars: 25 μm. Quantitative analysis of RYSV-infected cultured cells labeled with N-F antibodies at 72 h post RYSV inoculation, as revealed by confocal microscopy (1200 cells/condition were counted, mean ± SD; **$P < 0.01$). **b** RT-qPCR assay showing relative transcript levels of the *N*, *P*, *M*, and *P3* genes after different treatments. Data represent means ± SD and were analyzed using Student's *t*-test; *$P < 0.05$; **$P < 0.01$. **c** Immunoblot analysis of viral proteins from RYSV-infected VCMs with dsRNA treatments. N-, P-, M-, and P3-specific antibodies were used to detect the accumulation of different viral proteins at 84 hpi. Actin was used as the control and was detected with actin-specific antibody

file 1: Figure S2). These findings provide compelling evidence that *P3* knockdown impairs the establishment of viroplasms, which subsequently reduces RYSV infection in *N. cincticeps* cells.

To investigate the role of RYSV P3 in the viral infection of *N. cincticeps*, we microinjected dsP3 RNA mixed with RYSV crude extracts into third-instar nymphs. At 6 days post-injection, we labeled the alimentary canals of *N. cincticeps* with RYSV virion antibody and subjected them to immunofluorescence microscopy. In dsGFP-treated leafhoppers, RYSV was extensively distributed throughout the alimentary canal. In contrast, in dsP3-treated leafhoppers, RYSV was restricted to limited areas of the alimentary canal (Fig. 4a). Consistent with the results of immunofluorescence microscopy, RT-qPCR and immunoblotting assays confirmed that RYSV infection of *N. cincticeps* was significantly inhibited after dsP3 treatment (Fig. 4b, c). These findings suggest that P3 plays an

important role in viral infection in both VCMs and insect vectors.

RYSV N localizes to the nucleus via an importin α-dependent pathway

To elucidate the nuclear import pathway of N, we examined interactions between N and the nuclear import factor importin α of *N. cincticeps* using yeast two-hybrid assays. N specifically interacted with *N. cincticeps* importin α3, but not with importin α1 or importin α2 (Fig. 5a). This interaction was subsequently confirmed by a GST pulldown assay. These results suggest that RYSV N enters the nuclei of *N. cincticeps* cells via an importin α-dependent pathway involving importin α3 (Fig. 5b).

To further assess the role of importin α3 in the nuclear localization of RYSV N, ds importin α3 or ds GFP RNA was mixed with plasmids expressing a green fluorescent protein (GFP)-fused N protein and transfected into *N. cincticeps* culture cells. At 48 hpi, immunofluorescence
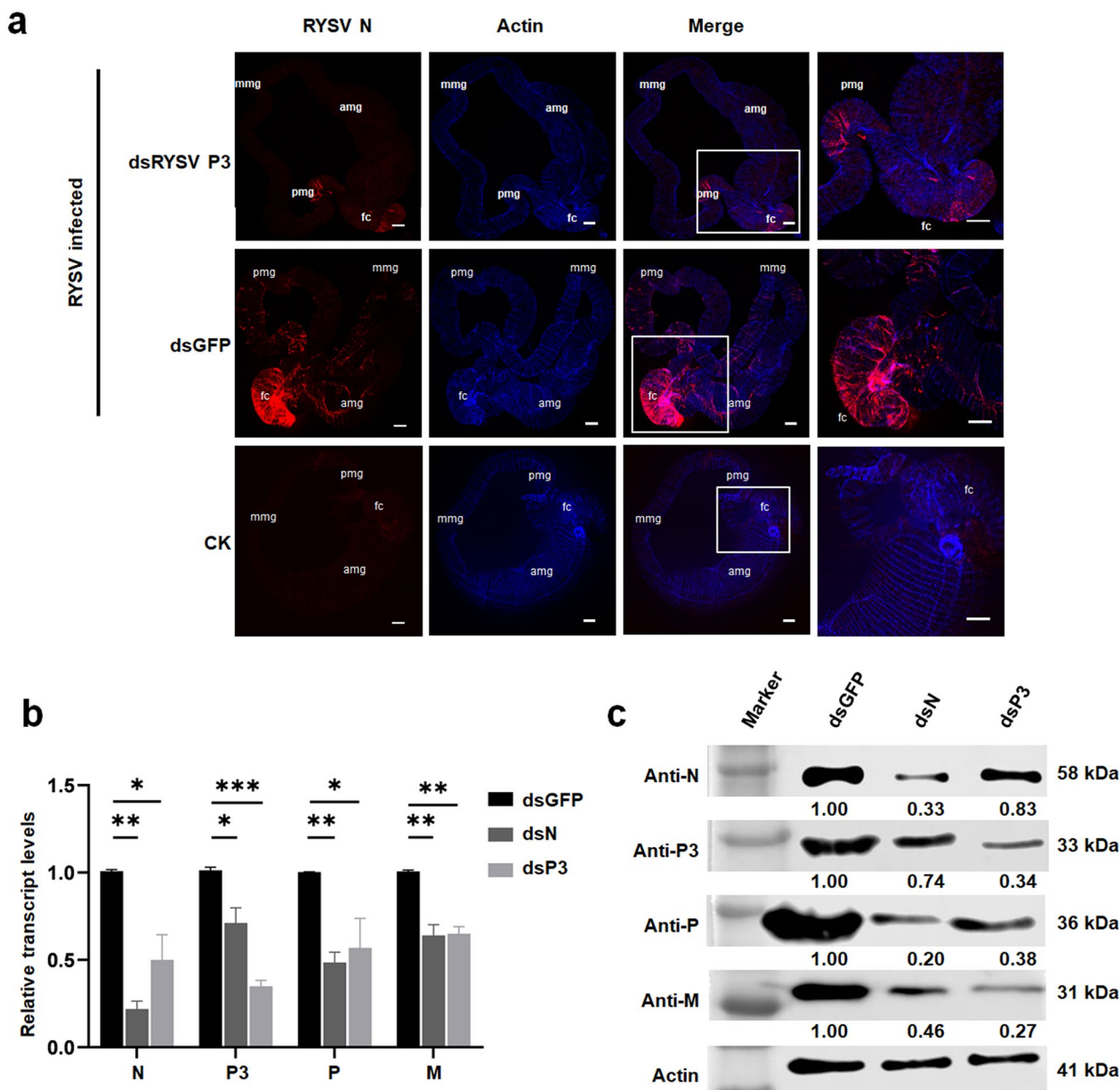
Fig. 4 Knockdown of *P3* by dsRNA treatment inhibits RYSV infection of leafhoppers. **a** Immunohistochemistry showing the variation in the amount of RYSV in midguts of nonviruliferous *N. cincticeps* at 6 days after injection with RYSV crude extracts and dsRNA of P3 and N. Nonviruliferous *N. cincticeps* were injected with dsGFP and RYSV crude extracts as a positive control. All samples were stained with RYSV-N-rhodamine and the actin dye phalloidin (blue). Scale bars: 100 μm. **b** RT-qPCR assay showing relative transcript levels of *N, P, M,* and *P3* after different dsRNA treatments. Three biological repeats were performed. Data represent means ± SD and were analyzed using Student's *t*-test; *$P < 0.05$; **$P < 0.01$. **c** The accumulation of viral proteins from *N. cincticeps* injected with RYSV crude extracts and dsP3 or dsN. N-, P-, M- and P3-specific antibodies were used to detect N, P, M, and P3 protein, respectively, at 84 hpi. Actin was used as the control and was detected with actin-specific antibody

microscopy revealed that the knockdown of *importin α3* resulted in the failure of N to enter the nucleus (Fig. 5c).

To determine the function of importin α3 during RYSV infection in insect vectors, we microinjected third-instar leafhoppers with a mixture of synthesized ds importin α3 RNA and RYSV virus solutions. At 7 dpi, RT-qPCR analysis showed that ds importin α3 treatment significantly decreased importin α3 expression in whole leafhopper bodies (Fig. 5d). Finally, we examined the transcription and expression of RYSV N, P3, P, and M using RT-qPCR and immunoblotting, respectively, finding that the knockdown of *importin α3* expression by

Huang *et al. Phytopathology Research*   (2023) 5:48

Page 7 of 11
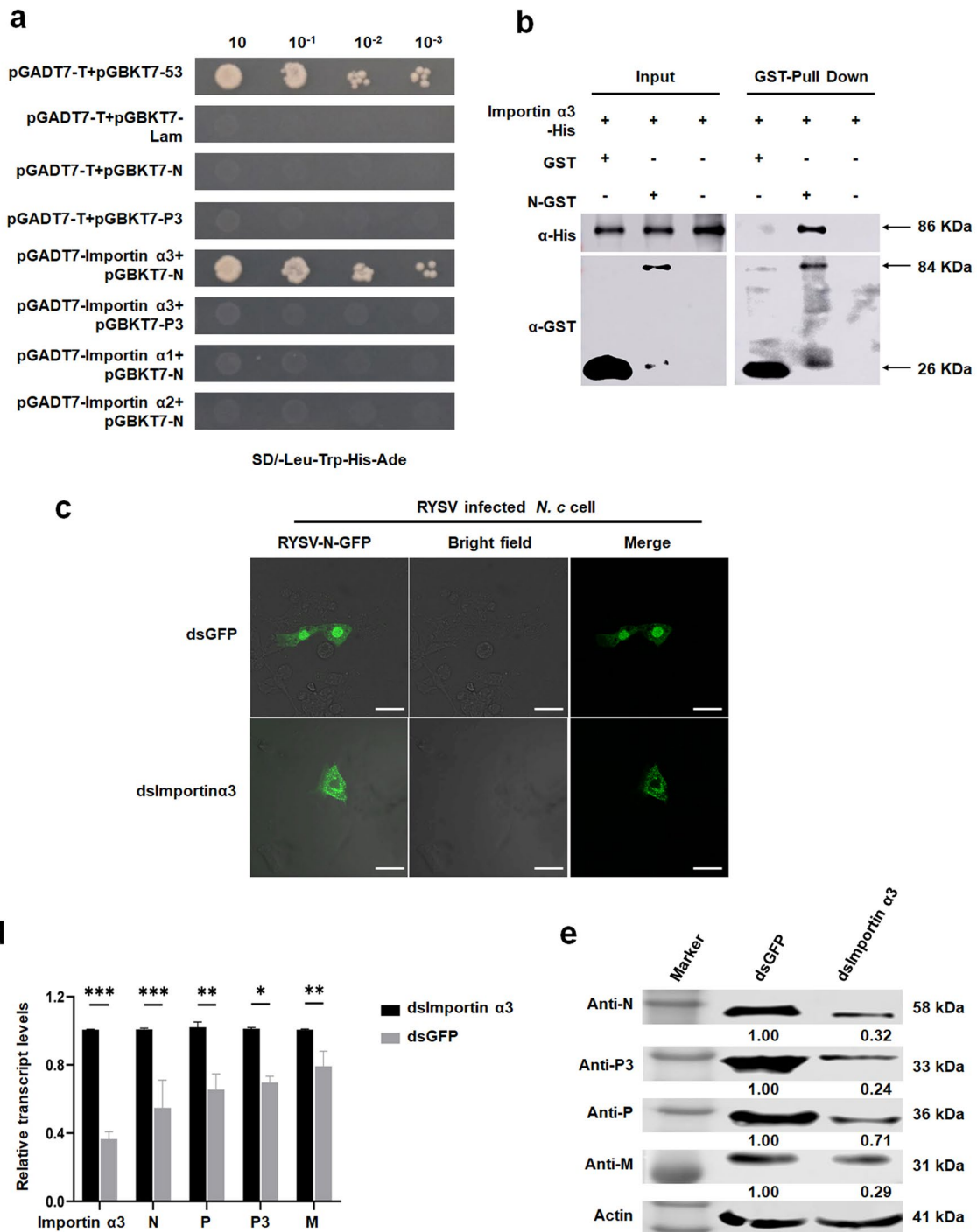
Fig. 5 RYSV N binds to importin α3 to enter the nucleus of the host cell. **a** Interactions of N and importin α1, importin α2, or importin α3, as determined using a yeast two-hybrid assay. Yeast cells co-transformed with pGBKT7–53 and pGADT7-T were used as a positive control. Yeast cells co-transformed with pGBKT7-Lam/pGADT7-T, pGBKT7-Importin α3/pGADT7-T were used as a negative control. **b** GST pull-down assay of the interaction of RYSV N with importin α3. Bait protein N was fused with GST-tagged protein. Prey protein importin α3 was fused with His-tagged protein. Purified GST incubated with prey protein and purified His incubated with bait protein were used as controls. **c** VCMs were transfected with dsP3 or importin α3 and inoculated with RYSV. At 72 h post RYSV inoculation, the cells were immunolabeled with N-specific IgGs directly conjugated to FITC. Scale bars: 25 μm. **d** RT-qPCR assay showing the relative transcript levels of the *N, P, M, P3*, and *importin α3* genes during RYSV infection of *N. cincticeps*. *N. cincticeps* cells were transfected with dsImportin α3 or dsGFP and then inoculated with RYSV. Three biological repeats were performed. Data represent means ± SD and were analyzed using Student's *t*-test; *$P < 0.05$; **$P < 0.01$. **e** Immunoblots of viral proteins from VCMs transfected with dsRNAs. N-, P-, M-, and P3-specific antibodies were used to detect N, P, M, and P3 protein, respectively, at 84 hpi. Actin was used as the control and was detected with actin-specific antibody

Huang *et al. Phytopathology Research*   (2023) 5:48

Page 8 of 11

RNAi suppressed RYSV infection in *N. cincticeps* (Fig. 5d, e).

Discussion

Members of the genus *Alphanucleorhabdovirus* assemble viroplasms and multiply in the nuclei of cells of both their host plants and insect vectors (Redinbaugh 2005; Ammar et al. 2009; Whitfield et al. 2018). The roles of nucleorhabdovirus proteins are well documented in host plants but not in insect vectors (Wang et al. 2015). We previously investigated the functions of RYSV N, P, P6, and M in insect cells (Wang et al. 2018; Zhang et al. 2018, 2021). In the present study, using a cultured leafhopper cell line, we demonstrated that the accessary protein P3 interacted with N in the viroplasms in the nuclei of leafhopper cells. Knocking down *P3* inhibited RYSV infection in both leafhopper cell cultures and the insect body. The import of P3 into the nucleus required its interaction with N via an importin α3-dependent pathway. Our findings provide evidence that P3 plays important roles in the infection of an insect vector by a plant alphanucleorhabdovirus.

The gene located between the *P* and *M* genes in the genomes of plant rhabdoviruses encodes a viral MP that helps form connections between neighboring plant cells to promote intercellular transport (Benitez-Alfonso et al. 2010). These MPs include Sonchus yellow net virus (SYNV) sc4, lettuce necrotic yellow virus 4b, RYSV P3, maize mosaic virus P3, and potato yellow dwarf virus (PYDV) Y protein (Scholthof et al. 1994; Huang et al. 2005; Reed et al. 2005; Tsai et al. 2005; Dietzgen et al. 2006; Heim et al. 2008; Massah et al. 2008; Bandyopadhyay et al. 2010). The previous investigation demonstrated that RYSV P3 is a member of the '30 K' superfamily of viral MPs. Heterologous expression of this protein complements the cell-to-cell movement of a movement-deficient plant virus; RYSV P3 moves through the plasmodesmata as an MP–nucleocapsid complex (Zhou et al. 2019). However, the role of RYSV P3 in the viral infection of insect cells remains unclear.

We observed that P3 was expressed in the cytoplasm of leafhopper cells during the early stage of RYSV infection and was then transported into the nucleus to form aggregates. Immunoelectron microscopy using P3-specific antibody confirmed the localization of P3 in RYSV viroplasms in the nuclei of leafhopper cells. Furthermore, knocking down *P3* inhibited the infection of the insect vector by RYSV. These findings suggest that P3 is involved in the assembly of RYSV viroplasms during RYSV infection of the insect vector. However, whether P3 protein performs the same function in plant cells requires further study. Furthermore, our findings do not rule out the possibility that RYSV also functions as an MP during the infection of insect cells.

There is no typical NLS in the P3 protein sequence, leading us to speculate that it may enter the nucleus through interactions with other RYSV proteins. Yeast two-hybrid experiments suggested that P3 interacts with N. Furthermore, immunofluorescence observations revealed that during the early stage of RYSV infection, P3 and N co-localize in the cytoplasm of leafhopper cells before jointly entering the nucleus to form the viral nucleocapsid. Therefore, the entry of P3 into the nucleus is facilitated through its interaction with N. Perhaps the nuclear entry of P3 in other plant rhabdoviruses follows a similar mechanism. Further investigations into the nuclear entry mechanisms of P3 proteins in different plant rhabdoviruses would provide valuable insights into their functions during viral infection.

The presence of NLSs within the N proteins of SYNV and PYDV has been experimentally established, confirming their interactions with importin-α and their roles in facilitating nuclear import (Goodin et al. 2001; Ghosh et al. 2008; Ruigrok et al. 2011). Computational analysis also predicted the existence of NLSs within the N protein of RYSV (Ghosh et al. 2008). In this study, we conducted a comprehensive investigation of the *N. cincticeps* genome, leading to the identification and cloning of three *importin α* genes. Through yeast two-hybrid and pull-down assays, we successfully validated the interaction between RYSV P3 and importin α3. When we employed dsRNA-mediated gene silencing to suppress the expression of *importin α* genes, we observed a notable impairment in the nuclear translocation of transiently expressed RYSV P3. Collectively, these findings provide compelling evidence supporting the essential role of the importin-mediated pathway in facilitating the nuclear import of RYSV N.

Conclusions

In the present study, we investigated the role of RYSV P3 in the viral infection of insect vectors. Our findings revealed that RYSV P3 is a constituent of viroplasms in the nuclei of leafhopper cells that plays a pivotal role in RYSV infection of *N. cincticeps*. W determined that P3 enters the nucleus through its interaction with N, which relies on importin α3-mediated nuclear import. The suppression of *importin α3* gene expression significantly inhibited RYSV infection within leafhoppers. These findings provide valuable insights into the mechanism underlying plant rhabdovirus infection in insect vectors.

Methods

Insects, cell culture, and reagents

Nonviruliferous leafhoppers (*N. cincticeps*) were collected from Yunnan Province in southern China and reared on rice seedlings in controlled environmental conditions. The leafhoppers were maintained in cages at

Huang *et al. Phytopathology Research*   (2023) 5:48

Page 9 of 11

28°C, relative humidity of 75 ± 5%, under a 16-h light/8-h dark cycle (Wang et al. 2018). Continuous monolayer cultures of *N. cincticeps* cells derived from embryonic medium were cryopreserved in liquid nitrogen and subsequently resuscitated in leafhopper vector cultured cells in monolayers (LBM) growth medium using established protocols. Once the cells reached confluency on coverslips, the original LBM growth medium was replaced with histidine-magnesium chloride solution (0.1 M histidine and 0.01 M MgCl$_2$, pH 6.2) and the cells were incubated for 5 min; this process was repeated three times.

To initiate viral infection, RYSV-infected rice leaves were diluted in histidine-magnesium chloride solution and inoculated onto leafhopper cells, which were incubated for 2 h. After removal of the inoculum, the infected cells were cultured in LBM growth medium for 48 h and analyzed by PCR. Antibodies specific to RYSV proteins were generated as previously described. Immunoglobulins G (IgGs) were purified from the respective polyclonal antibodies and conjugated directly to FITC, rhodamine, or Alexa Fluor 633 (Invitrogen) following the manufacturer's instructions.

Immunofluorescence microscopy
RYSV-infected VCMs or the model cell line *Spodoptera frugiperda* (Sf9) infected with recombinant baculoviruses were grown on glass coverslips. Leafhopper salivary glands and midguts were dissected on a glass plate using 0.01 M phosphate-buffered saline (PBS). The samples were fixed in 4% paraformaldehyde for 1 h at 37°C and subsequently permeabilized with 0.2% Triton X-100. Following three washes with PBS, the samples were incubated overnight at 4°C with lab-made IgG antibodies. Fluorescence was observed under a Leica TCS SP5 inverted confocal microscope.

Baculovirus expression assay
The subcellular localizations of RYSV N and P3 in Sf9 cells were investigated using the baculovirus expression system. RYSV N was engineered into a recombinant shuttle plasmid with a His-tag (N-His), and RYSV P3 was tagged with Strep (P3-Strep). Each recombinant shuttle plasmid was transformed into *Escherichia coli* DH10 Bac competent cells (Invitrogen, USA). The resulting recombinant shuttle plasmids were transfected (separately or together) into Sf9 cells using Cellfectin II Reagent (Thermo Fisher Scientific, USA). At 3 days after transfection, the cell culture supernatant was collected and used to infect healthy Sf9 cells for 48 h. The infected cells were fixed in 4% paraformaldehyde and immunolabeled using antibodies specific to His-tag and Strep-tag conjugated to FITC

or rhodamine. Finally, the cells were observed under an immunofluorescence microscope.

Transmission electron microscopy
Both healthy and RYSV-infected *N. cincticeps* cells were fixed, dehydrated, and embedded following previously established protocols. Ultrathin sections were prepared as described. For immunoelectron microscopy, the VCM samples were incubated with N- or P3-specific IgGs as the primary antibody (diluted 1:50). Subsequently, the samples were labeled with goat anti-rabbit IgG conjugated with 15-nm gold particles or goat anti-mouse IgG conjugated with 10-nm gold particles as the secondary antibody (diluted 1:100, Sigma). The labeled ultrathin sections were examined under an H-7650 Hitachi transmission electron microscope.

Yeast two-hybrid assay
To investigate the interactions between RYSV P3 and other viral proteins, yeast two-hybrid screening was conducted using the Matchmaker Gal4 Two-Hybrid System 3. The *P3* gene of RYSV was cloned into the bait plasmid pGBKT7 (pGBKT7-P3), and the genes encoding the other viral proteins were inserted into the prey vector pGADT7 (pGADT7-N, pGADT7-M, pGADT7-P, pGADT7-G). Each combination of bait and prey plasmids, along with the positive control (pGBKT7-53/pGADT7-T) and negative control (pGBKT7-Lam/pGADT7-T), was co-transformed into yeast strain AH109. The transformants were cultured on selective SD/−Leu/−Trp medium for 3–4 days at 30°C. Single colonies were selected and streaked onto SD/−Leu/−Trp/−His/−Ade/X-α-gal medium to assess protein−protein interactions. The interactions of RYSV N and P3 with importin α1, α2, and α3 were examined using the same method.

GST pull-down assay
The interaction between RYSV N and RYSV P3 was confirmed using the GST pull-down system. The ORF of RYSV *N* was cloned into the pGEX-4 T vector to enable the fusion of N protein with GST-tag. Likewise, the ORFs of RYSV *P3* and importin *α3* were cloned into pET-28b for fusion with His-tag. All three recombinant plasmids were expressed in *E. coli* strain BL21. Lysates containing GST-N were incubated with Glutathione Sepharose 4B beads at 4°C for 4 h. Subsequently, the beads were rinsed with 0.01 M PBS to remove excess proteins and incubated with purified P3-His or importin α3-His recombinant proteins for an additional 4 h at 4°C. The mixtures were washed with elution buffer and analyzed by immunoblotting using GST-tag and His-tag antibodies, respectively.

Huang *et al. Phytopathology Research* (2023) 5:48

Page 10 of 11

RT-qPCR

To evaluate the expression of RYSV genes following the knockdown of *N, P3,* and *importin α3*, the cell was collected for total RNA extraction. Subsequently, an RT-qPCR assay was performed using a SYBR Green PCR Master Mix kit (Promega, Madison, WI, USA). The *Actin* gene was used as the internal control. Relative gene expression levels were determined using the $2^{-\Delta\Delta CT}$ method.

Knocking down the in vivo expression of *N, P,* and *importin α3* in RYSV-infected *N. cincticeps*

Double-stranded RNAs (dsRNAs) targeting the *N, P3, importin α3,* and *GFP* genes were synthesized following the manufacturer's instructions as previously described. Equal volumes of RYSV crude extracts and the dsRNA mixture were microinjected into the abdomens of non-viruliferous third- or fourth-instar nymphs. At 6 days post-microinjection, salivary glands and midguts were dissected for immunohistochemistry assays. The antibodies used for immunostaining and their respective dilutions were as follows: anti-N (1:100) and anti-actin (1:85). In addition, RT-qPCR and immunoblotting were employed to assess the accumulation of N, P, M, and P3 proteins. RT-qPCR assays were performed in triplicate and analyzed using Student's t-test for statistical analysis.

Statistical analyses

All data were analyzed for statistical differences using SPSS (version 19.0; SPSS, USA). Multiple comparisons of the means were conducted using one-way analysis of variance and Tukey's honest significant difference (HSD) test at the $P < 0.05$ significance level.

Abbreviations

amg	Anterior midgut
fc	Filter chamber
FITC	Fluorescein isothiocyanate
GFP	Green fluorescent protein
GST	Glutathione-S-transferase
hpi	Hours post-infection
IgG	Immunoglobulin G
LBM	Leafhopper vector cultured cells in monolayers
mmg	Middle midgut
MP	Movement protein
NLS	Nuclear localization signal
Nu	Nucleus
ORF	Open reading frame
PBS	Phosphate-buffered saline
pmg	Posterior midgut
PYDV	Potato yellow dwarf virus
RNAi	RNA interference
RYSV	Rice yellow stunt virus
Sf9	*Spodoptera frugiperda* Cells
SYNV	Sonchus yellow net virus
VCM	Vector cell monolayer
Vp	Viroplasm

Supplementary Information

Additional file 1: Figure S1. GST pull-down assay of the interaction of RYSV P3 with RYSV M. **Figure S2.** RT-qPCR assay showing relative transcript levels of the N, P, P3, and M genes after ds3'UTR treatments.

Availability of data and materials
Not applicable.

Declarations

Ethics approval and consent to participate
Not applicable.

Consent for publication
Not applicable.

Competing interests
The authors declare that they have no competing interests.

References

Ammar E-D, Tsai CW, Whitfield AE, Redinbaugh MG, Hogenhout SA. Cellular and molecular aspects of rhabdovirus interactions with insect and plant hosts. Annu Rev Entomol. 2009;54:447–68. https://doi.org/10.1146/annurev.ento.54.110807.090454.

Bandyopadhyay A, Kopperud K, Anderson G, Martin K, Goodin M. An integrated protein localization and interaction map for Potato yellow dwarf virus, type species of the genus Nucleorhabdovirus. Virology. 2010;402:61–71.

Benitez-Alfonso Y, Faulkner C, Ritzenthaler C, Maule AJ. Plasmodesmata: gateways to local and systemic virus infection. Mol Plant Microbe Interact. 2010;23:1403–12.

Cheng ZX, Ruan YL, Cheng DD. Rice yellow stunt virus occurrence and prevalence. J Plant Protec. 1992;4:33–4. https://doi.org/10.1146/annurev.phyto.34.1.249.

Dietzgen RG, Callaghan B, Wetzel T, Dale JL. Completion of the genome sequence of Lettuce necrotic yellows virus, type species of the genus Cytorhabdovirus. Virus Res. 2006;118:16–22. https://doi.org/10.1016/j.virusres.2005.10.024.

Ding ZH, Gao Q, Tong X, Xu WY, Ma L, Zhang ZJ, et al. MAPKs trigger antiviral immunity by directly phosphorylating a rhabdovirus nucleoprotein in plants and insect vectors. Plant Cell. 2022;34:3110–27. https://doi.org/10.1093/plcell/koac143.

Fang RX, Wang Q, Xu BY, Pang Z, Zhu HT, Mang KQ, et al. Structure of the nucleocapsid protein gene of rice yellow stunt rhabdovirus. Virology. 1994;204:367–75. https://doi.org/10.1006/viro.1994.1541.

Fang XD, Gao Q, Zang Y, Qiao JH, Gao DM, Xu WY, et al. Host casein kinase 1-mediated phosphorylation modulates phase separation of a rhabdovirus phosphoprotein and virus infection. Elife. 2022;11:e74884. https://doi.org/10.7554/eLife.74884.

Gao Q, Xu WY, Yan T, Fang XD, Cao Q, Zhang ZJ, et al. Rescue of a plant cytorhabdovirus as versatile expression platforms for planthopper and cereal genomic studies. New Phytol. 2019;223:2120–33. https://doi.org/10.1111/nph.15889.

Gao DM, Zhang ZJ, Qiao JH, Gao Q, Zang Y, Xu WY, et al. A rhabdovirus accessory protein inhibits jasmonic acid signaling in plants to attract insect vectors. Plant Physiol. 2022;190:1349–64. https://doi.org/10.1093/plphys/kiac319.

Ghosh D, Brooks RE, Wang R, Lesnaw J, Goodin MM. Cloning and subcellular localization of the phosphoprotein and nucleocapsid proteins of Potato yellow dwarf virus, type species of the genus Nucleorhabdovirus. Virus Res. 2008;135:26–35. https://doi.org/10.1016/j.virusres.2008.02.003.

Goodin MM, Austin J, Tobias R, Fujita M, Morales C, Jackson AO. Interactions and nuclear import of the N and P proteins of sonchus yellow net virus, a plant nucleorhabdovirus. J Virol. 2001;75:9393–406. https://doi.org/10.1128/jvi.75.19.9393-9406.2001.

Guo H, Song X, Xie C, Huo Y, Zhang F, Chen X, et al. Rice yellow stunt rhabdovirus protein 6 suppresses systemic RNA silencing by blocking RDR6-mediated secondary siRNA synthesis. Mol Plant Microbe Interact. 2013;26:927–36. https://doi.org/10.1094/mpmi-02-13-0040-r.

Heim F, Lot H, Delecolle B, Bassler A, Krczal G, Wetzel T. Complete nucleotide sequence of a putative new cytorhabdovirus infecting lettuce. Arch Virol. 2008;153:81–92. https://doi.org/10.1007/s00705-007-1071-5.

Hogenhout SA, et al. Insect vector interactions with persistently transmitted viruses. Annu Rev Phytopathol. 2008;46:327–59. https://doi.org/10.1146/annurev.phyto.022508.092135.

Huang Y, Zhao H, Luo Z, Chen X, Fang RX. Novel structure of the genome of Rice yellow stunt virus: identification of the gene 6-encoded virion protein. J Gen Virol. 2003;84:2259–64. https://doi.org/10.1099/vir.0.19195-0.

Huang YW, Geng YF, Ying XB, Chen XY, Fang RX. Identification of a movement protein of rice yellow stunt rhabdovirus. J Virol. 2005;79:2108–14.

Jackson AO, Li Z. Developments in plant negative-Strand RNA virus reverse genetics. Annu Rev Phytopathol. 2016;54:469–98. https://doi.org/10.1146/annurev-phyto-080615-095909.

Kormelink R, Garcia ML, Goodin M, Sasaya T, Haenni AL. Negative-strand RNA viruses: the plant-infecting counterparts. Virus Res. 2011;162:184–202. https://doi.org/10.1016/j.virusres.2011.09.028.

Kuhn JH, Adkins S, Alioto D, Alkhovsky SV, Amarasinghe GK, Anthony SJ, et al. 2020 taxonomic update for phylum Negarnaviricota (Riboviria: Orthornavirae), including the large orders Bunyavirales and Mononegavirales. Arch Virol. 2020;165:3023–72. https://doi.org/10.1007/s00705-020-04731-2.

Kuzmin IV, Novella IS, Dietzgen RG, Padhi A, Rupprecht CE. The rhabdoviruses: biodiversity, phylogenetics, and evolution. Infect Genet Evol. 2009;9:541–53. https://doi.org/10.1016/j.meegid.2009.02.005.

Mann KS, Dietzgen RG. Plant rhabdoviruses: new insights and research needs in the interplay of negative-strand RNA viruses with plant and insect hosts. Arch Virol. 2014;159:1889–900. https://doi.org/10.1007/s00705-014-2029-z.

Massah A, Izadpanah K, Afsharifar AR, Winter S. Analysis of nucleotide sequence of Iranian maize mosaic virus confirms its identity as a distinct nucleorhabdovirus. Arch Virol. 2008;153:1041–7. https://doi.org/10.1007/s00705-008-0085-y.

Melcher U. The "30K" superfamily of viral movement proteins. J Gen Virol. 2000;81:257–66. https://doi.org/10.1099/0022-1317-81-1-257.

Redinbaugh MG, Hogenhout SA. Plant rhabdoviruses. Curr Top Microbiol Immunol. 2005;292:143–63. https://doi.org/10.1007/3-540-27485-5_7.

Reed SE, Tsai CW, Willie KJ, Redinbaugh MG, Hogenhout SA. Shotgun sequencing of the negative-sense RNA genome of the rhabdovirus Maize mosaic virus. J Virol Methods. 2005;129:91–6. https://doi.org/10.1016/j.jviromet.2005.05.013.

Ruigrok RW, Crépin T, Kolakofsky D. Nucleoproteins and nucleocapsids of negative-strand RNA viruses. Curr Opin in Microbiol. 2011;14:504–10. https://doi.org/10.1016/j.mib.2011.07.011.

Scholthof KB, Hillman BI, Modrell B, Heaton LA, Jackson AO. Characterization and detection of sc4: a sixth gene encoded by sonchus yellow net virus. Virology. 1994;204:279–88. https://doi.org/10.1006/viro.1994.1532.

Tsai CW, Redinbaugh MG, Willie KJ, Reed S, Goodin M, Hogenhout SA. Complete genome sequence and in planta subcellular localization of maize fine streak virus proteins. J Virol. 2005;79:5304–14. https://doi.org/10.1128/jvi.79.9.5304-5314.2005.

Wang Q, Ma X, Qian S, Zhou X, Sun K, Chen X, et al. Rescue of a plant negative-strand RNA virus from cloned cDNA: insights into enveloped plant virus movement and morphogenesis. PLoS Pathog. 2015;11:e1005223. https://doi.org/10.1371/journal.ppat.1005223.

Wang H, Wang J, Xie Y, Fu Z, Wei T, Zhang XF. Development of leafhopper cell culture to trace the early infection process of a nucleorhabdovirus, rice yellow stunt virus, in insect vector cells. Virol J. 2018;15:72. https://doi.org/10.1186/s12985-018-0987-6.

Whitfield AE, Huot OB, Martin KM, Kondo H, Dietzgen RG. Plant rhabdoviruses-their origins and vector interactions. Curr Opin Virol. 2018;33:198–207. https://doi.org/10.1016/j.coviro.2018.11.002.

Zhang XF, Xie Y, Wang H, Wang J, Chen H, Zeng T, et al. Exploration of an actin promoter-based transient expression vector to trace the cellular localization of nucleorhabdovirus proteins in leafhopper cultured cells. Front Microbiol. 2018;9:3034. https://doi.org/10.3389/fmicb.2018.03034.

Zhang XF, Zeng T, Xie Y, Zheng Y, Wang H, Lin H, et al. Rice yellow stunt virus activates polyamine biosynthesis to promote viral propagation in insect vectors by disrupting ornithine decarboxylase antienzyme function. Sci China Life Sci. 2021;64:1522–32. https://doi.org/10.1007/s11427-020-1846-8.

Zhou X, Lin W, Sun K, Wang S, Zhou X, Jackson AO, et al. Specificity of plant rhabdovirus cell-to-cell movement. J Virol. 2019;93:e00296-e319. https://doi.org/10.1128/jvi.00296-19.

Zhou X, Sun K, Zhou X, Jackson AO, Li Z. The matrix protein of a plant rhabdovirus mediates superinfection exclusion by inhibiting viral transcription. J Virol. 2019;93:00680–719.